

การสังเคราะห์และวิเคราะห์อนุภาคนาโนของทองเหลือง
โดยวิธีอาร์คดิสชาร์ตสำหรับหมึกนำไฟฟ้า

นางสาวราชวิ สว่างหล้า

วิทยานิพนธ์นี้เป็นส่วนหนึ่งของการศึกษาตามหลักสูตรปริญญาวิทยาศาสตรมหาบัณฑิต
สาขาวิชาวิศวกรรมเคมี ภาควิชาวิศวกรรมเคมี
คณะวิศวกรรมศาสตร์ จุฬาลงกรณ์มหาวิทยาลัย
ปีการศึกษา 2555
ลิขสิทธิ์ของจุฬาลงกรณ์มหาวิทยาลัย

บทคัดย่อและแฟ้มข้อมูลฉบับเต็มของวิทยานิพนธ์ตั้งแต่ปีการศึกษา 2554 ที่ให้บริการในคลังปัญญาจุฬาฯ (CUIR)
เป็นแฟ้มข้อมูลของนิสิตเจ้าของวิทยานิพนธ์ที่ส่งผ่านทางบัณฑิตวิทยาลัย

The abstract and full text of theses from the academic year 2011 in Chulalongkorn University Intellectual Repository (CUIR)
are the thesis authors' files submitted through the Graduate School.

SYNTHESIS AND CHARACTERIZATION OF BRASS NANOPARTICLES
BY ARC DISCHARGE METHOD FOR CONDUCTIVE INK

Miss Rachawee Savanglaa

A Thesis Submitted in Partial Fulfillment of the Requirements
for the Degree of Master of Engineering Program in Chemical Engineering

Department of Chemical Engineering

Faculty of Engineering

Chulalongkorn University

Academic Year 2012

Copyright of Chulalongkorn University

Thesis Title SYNTHESIS AND CHARACTERIZATION OF BRASS
 NANOPARTICLES BY ARC DISCHARGE METHOD FOR
 CONDUCTIVE INK

By Miss Rachawee Savanglaa

Field of Study Chemical Engineering

Thesis Advisor Assistant Professor Soorathep Kheawhom, Ph.D.

Accepted by the Faculty of Engineering, Chulalongkorn University in Partial Fulfillment
of the Requirements for the Master's Degree

.....Dean of the Faculty of Engineering
(Associate Professor Boonsom Lerthirunwong, Dr.Ing.)

THESIS COMMITTEE

.....Chairman

(Professor Piyasan Prasertdam, Dr.Ing.)

.....Thesis Advisor
(Assistant Professor Soorathep Kheawhom, Ph.D.)

.....Examiner
(Assistant Professor Anongnat Somwangthanaroj, Ph.D.)

.....Examiner
(Associate Professor Supakanok Thongyai, Ph.D.)

.....External Examiner
(Assistant Professor Sirirat Wacharawichanant, D.Eng.)

รชาวี สว่างหล้า : การสังเคราะห์และวิเคราะห์อนุภาคนาโนของทองเหลืองโดยวิธีอาร์ค
 ดิสชาร์ตสำหรับหมึกนำไฟฟ้า. (SYNTHESIS AND CHARACTERIZATION OF BRASS
 NANOPARTICLES BY ARC DISCHARGE METHOD FOR CONDUCTIVE INK)

อ.ที่ปรึกษาวิทยานิพนธ์หลัก: ผศ.ดร.สุรเทพ เขียวหอม, 48 หน้า.

วิทยานิพนธ์เล่มนี้เสนอการสังเคราะห์อนุภาคนาโนของทองเหลืองโดยวิธีอาร์คดิสชาร์ต
 (Arc discharge) ในของเหลวที่เป็นฉนวนไฟฟ้าต่างกัน 3 ชนิด คือ น้ำกลั่นปราศจากไอออน เอทิลีน
 ไกลคอล (Ethylene glycol) และเอทานอล (Ethanol) ที่สภาวะความดันบรรยากาศปกติ โครงสร้าง
 ขนาด และรูปร่างของอนุภาคที่สังเคราะห์ได้ถูกวิเคราะห์โดย XRD SEM และ TEM ตามลำดับ
 พบว่าอนุภาคที่สังเคราะห์ได้ในของเหลวที่เป็นฉนวนไฟฟ้าทั้ง 3 ชนิดประกอบด้วยทองเหลือง
 (CuZn) และออกไซด์ของสังกะสี (ZnO) ซึ่งเกิดจากการทำปฏิกิริยากับอนุมูลอิสระของออกซิเจนที่
 เกิดขึ้นในระหว่างการสลายตัวของของเหลวที่เป็นฉนวนไฟฟ้า อนุภาคที่สังเคราะห์ได้มีขนาด 10.9
 nm ในเอทิลีนไกลคอล, 17.3 nm ในเอทานอล และ 95.1 nm ในน้ำกลั่นปราศจากไอออน นอกจากนี้
 ได้ศึกษาผลของการเติมกรดแอสคอร์บิกเข้มข้น 0.1 M ลงในสารละลายคอลลอยด์ที่สังเคราะห์ได้
 จากของเหลวที่เป็นฉนวนไฟฟ้าทั้ง 3 ชนิดพบว่า สามารถรีดิวซ์อนุภาคออกไซด์ของสังกะสีในน้ำ
 ปราศจากไอออนและเอทิลีนไกลคอลได้ แต่ในเอทานอลจะเกิดอนุภาคของซิงค์ออกซาลาต (Zinc
 oxalate hydrate) ขึ้น การศึกษาผลของปริมาณทองเหลืองที่อาร์คลงไปทีปริมาณ 3.47, 6.95 และ
 10.43 กรัมต่อลิตร พบว่าอนุภาคที่สังเคราะห์ได้มีขนาดไม่แตกต่างกันอย่างมีนัยสำคัญ ดังนั้นใน
 งานวิจัยนี้จึงนำอนุภาคที่สังเคราะห์ได้จากการอาร์คทองเหลือง 10.43 กรัมต่อลิตรในเอทิลีนไกล
 คอลและเติมกรดแอสคอร์บิก 0.1 M มาเตรียมหมึกทองเหลืองนำไฟฟ้า และพิมพ์ลงบนแผ่น PET
 ด้วยวิธีการสกรีน จากนั้นนำไปเผาผนึก (sintering) ภายใต้อุณหภูมิของกรดฟอร์มิคที่อุณหภูมิ 150 องศา
 เซลเซียสเป็นเวลา 30, 60, 90, 120 และ 480 นาที จากการตรวจสอบด้วย SEM แสดงให้เห็นว่า
 อนุภาคเริ่มหลอมเมื่อเวลาผ่านไป 30 นาที และความต้านทานไฟฟ้าจะลดลงเมื่อเวลาการเผาผนึก
 เพิ่มขึ้น โดยความต้านทานไฟฟ้าที่น้อยที่สุดเท่ากับ 22.05 โอห์มเซนติเมตร

ภาควิชา..... วิศวกรรมเคมี..... ลายมือชื่อนิสิต.....
 สาขาวิชา..... วิศวกรรมเคมี..... ลายมือชื่อ อ.ที่ปรึกษาวิทยานิพนธ์หลัก.....
 ปีการศึกษา..... 2555.....

5470339021 : MAJOR CHEMICAL ENGINEERING

KEYWORDS : BRASS/NANOPARTICLE/ARC DISCHARGE/CONDUCTIVE INK

RACHAWEE SAVANGLAA : SYNTHESIS AND CHARACTERIZATION OF BRASS
NANOPARTICLES BY ARC DISCHARGE METHOD FOR CONDUCTIVE INK.

ADVISOR : ASST. PROF. SOORATHEP KHEAWHOM, Ph.D., 48 pp.

This research proposes the synthesis approach of copper-zinc nanoparticles by using arc discharge submerged in three different dielectric liquids including ethylene glycol, water, and ethanol at ambient atmosphere. The particles size, microstructure and morphology of particles were characterized via transmission electron microscopy (TEM), Scanning electron microscope (SEM) and X-ray diffraction (XRD), respectively. The nanoparticles synthesized in three different dielectric liquids contain both copper-zinc and zinc oxide. The zinc oxide was formed by oxygen free radicals during decomposition of the dielectric liquid. The average size of the nanoparticles synthesized in ethylene glycol, ethanol and deionized water estimated by Scherrer's equation were 10.9 nm, 17.3 nm, and 95.1 nm, respectively. In addition, we studied the effect of L-ascorbic acid with concentration of 0.1 M as reducing agent. L-ascorbic acid could reduce zinc oxide particles in deionized water and ethylene glycol. In ethanol, zinc oxalate was formed after adding L-ascorbic acid. In order to study effect of amount of brass loading into dielectric liquids, we used 3.47, 6.95, and 10.43 gram/liter of brass loading. The nanoparticles are slightly increased as the amount of brass loading increases. Thus, we used 10.43 gram/liter of brass synthesized in ethylene glycol with ascorbic acid 0.1 M to prepared conductive ink. The pattern was printed on coated PET film by screen printing. Then, the pattern printed was baked at 150°C with formic acid vapor for 30, 60, 90, 120 and 480 minute. The SEM images show the nanoparticles starting to melt after sintering for 30 minute and the electric resistivity decreases with the increase of the sintering time. The minimum electrical resistivity obtained was 22.05 Ω cm.

Department : Chemical Engineering Student's Signature

Field of Study : Chemical Engineering Advisor's Signature

Academic Year : .. 2012

ACKNOWLEDGEMENTS

I would like to sincere thank my advisor, Asst. Prof. Soorathep Kheawhom for active interest and inspiring guidance in my work. I would like to express my gratitude to my thesis committee, Professor Dr. Piyasan Prasertdam, Assistant Professor Dr. Anongnat Somwangthanaroj, Associate Professor Supakanok Thongyai and Assistant Professor Sirirat Wacharawichanant for helpful suggestions and insightful comments. I sincerely thank Mektec Manufacturing Corporation (Thailand) Ltd. for financial supporting along with materials and equipments for characterizations in my research. Finally, I am forever indebted to my parents for their support.

CONTENTS

	Page
ABSTRACT IN THAI.....	iv
ABSTRACT IN ENGLISH.....	v
ACKNOWLEDGEMENTS.....	vi
CONTENTS.....	vii
LIST OF TABLES.....	ix
LIST OF FIGURES.....	x
CHAPTER I INTRODUCTION.....	1
1.1 Background and motivation.....	1
1.2 Objective of the research.....	2
1.3 Scope of the research.....	2
1.4 Expected benefits.....	3
CHAPTER II FUNDAMENTAL.....	4
2.1 Nanoparticles.....	4
2.2 Alloy.....	4
2.3 Brass.....	5
2.2.1 Property.....	5
2.2.2 Type.....	6
2.4 Electric arc discharge.....	7
2.5 Reduction-oxidation reaction.....	8
2.6 Conductive ink.....	9
2.7 Substrate.....	10
2.8 Sintering.....	10
CHAPTER III LITERATURE REVIEWS.....	12
CHAPTER IV EXPERIMENTAL.....	18
4.1 Materials.....	22
4.2 Synthesis of nanoparticles by arc discharge method.....	18
4.2.1 Effect of dielectric liquid.....	19

	Page
4.2.2 Effect of reducing agent.....	20
4.2.3 Effect of metal loading.....	20
4.3 Preparation of conductive ink.....	21
4.4 Screen printing.....	21
4.5 Reactive sintering of formic acid vapor reduction.....	22
4.6 Characterization.....	22
CHAPTER V RESULT AND CONCUSSION.....	23
5.1 Synthesis of nanoparticles by arc discharge in different dielectric liquid.....	23
5.2 Effect of reducing agents on the synthesized particles.....	28
5.3 Effect of brass loading on the synthesized particles.....	31
5.4 Printed and sintering processes.....	35
CHAPTER VI CONCLUSIONS.....	40
6.1 Conclusions.....	40
6.2 Recommendations.....	41
REFERENCES.....	42
VITA.....	48

LIST OF TABLES

Table		Page
2.1	The list of common brass alloys.....	6
4.1	The experimental conditions to investigate effect of dielectric liquid	19
4.2	The experimental conditions to investigate effect of reducing agent.....	20
4.3	The experimental conditions to investigate effect of brass loading.....	21
5.1	Amounts of brass loading into ethylene glycol and concentration of colloid solution	31
5.2	The compositions of conductive ink.....	35
5.3	The resistivity of the screen printed pattern using brass ink on coated PET substrate.....	39

LIST OF FIGURES

Figure		Page
2.1	Schematic of electric discharge machining	7
2.2	Schematic of redox reaction.....	8
2.3	Developments of the microstructures by sintering.....	11
3.1	XRD spectra of oxide scale formed on the specimens after oxidation at different oxidation temperature for 3 h. showing that oxide is hexagonal ZnO.....	13
3.2	Schematic of screen printing process.....	17
4.1	Schematic diagram of the Arc discharge system.....	19
4.2	Schematic diagram of screen printed	22
5.1	Plasma of arc discharge.....	23
5.2	XRD patterns of particles synthesized in different dielectric liquids	24
5.3	SEM image of particles synthesized in different dielectric liquids	25
5.4	TEM images of particles synthesized in different dielectric liquids	26
5.5	XRD patterns of particles synthesized in different dielectric liquids after added ascorbic acid	28
5.6	SEM image of particles synthesized in different dielectric liquids after adding ascorbic acid	29
5.7	TEM images of particles synthesized in different dielectric liquids after adding ascorbic acid	30
5.8	XRD patterns of nanoparticles synthesized in different amount of brass loading	32
5.9	XRD patterns of nanoparticles synthesized in different amount of brass loading after added ascorbic acid.....	32
5.10	SEM image of nanoparticles synthesized in different amount of brass loading.....	33

	Page
5.11 TEM image of nanoparticles synthesized in different concentration of brass loading	34
5.12 The screen printed pattern using brass ink on coated PET substrate	35
5.13 XRD pattern of the printed pattern using brass ink on coated PET film before and after sintering	36
5.14 EDX pattern of the screen printed pattern using brass ink on coated PET film	37
5.15 SEM images of the printed pattern using brass ink on coated PET film before and after sintering.....	38
5.16 The printed pattern using brass ink on coated PET film after sintering at 150 °C for 480 min.....	39

CHAPTER I

INTRODUCTION

1.1 Background and motivation

Recently, flexible and printed electronic devices have been developed and draw a lot of attention. Because, It can be applied to generate various innovative products such as printed antennas, large area displays, flexible photovoltaic cells, and thin and flexible batteries (Tai et al, 2011; Faddoul et al., 2012 and Tang et al., 2010). One important component for a flexible electronics is a conductive layer with high electrical conductivity and stability. Generally, the conductive layer is fabricated by printing of metal nanoparticle conductive inks (Tai et al, 2011 and Russo et al., 2011). Silver is the highest conductive metal and usually used as a main ingredient for conductive inks. Silver is not only the most highly conductive metal, but it is also stable under ambient condition. Moreover, its oxide is electrically conductive (Kamyshny et al., 2011). Further, silver inks are curable at low temperatures. However, silver is costly to be produced and used in most cases.

Copper is one alternate metal that can replace silver because it is cheaper and its conductivity is the second highest of any metals. However, copper, especially in nano form, is prone to form oxide in atmospheric condition, and copper oxide is not electrically conductive. Moreover, copper oxide requires high sintering temperature (Tang et al, 2010). Consequently, sophisticated conditions are required to fabricate and process copper inks.

In order to protect the copper nanoparticles from oxidation, a number of approaches have been proposed, for example, graphitic, polymeric or ligand coatings. These coating materials will hinder inter-particle contact and hence conductivity unless removed in a subsequent sintering step. Therefore, the main objective of this research is to improve the stability of copper nanoparticles by adding second metal in a form of a copper alloy. Alloy nanoparticles consist of two or more metals with a potential to form compositionally order phases. They have some properties different from those bulk materials such as low density, and high strength (Kassae et al., 2008 and Pithawalla et al, 2003). Alloy nanoparticles have become of interest because we can control the composition, crystalline phase and morphology of nanoparticles to develop new nanophase materials with unique properties for many applications.

A number of techniques have been used to synthesize alloy nanoparticles. These techniques include wet chemical, laser vaporization and arc method. The laser vaporization controlled condensation is another technique to synthesis alloy nanoparticles. This technique relies on the principles of nucleation from vapor phase containing a mixture of the metal atoms of interest in the presence of an inert carrier gas (Pithawalla et al., 2003). Arc discharge method is a fast, simple, clean, and easily adaptable to mass production of nanoparticles (Tien et al., 2010; Lo et al., 2007; Kassaei et al., 2009-2010 and Hosseynizadeh et al., 2012). When arc discharge occurs between two electrodes, the metal layers are vaporized and condensed into dielectric liquid.

In this study, we investigate the synthesis of copper-zinc (brass) nanoparticles by using arc discharge submerged in various different dielectric liquids including ethylene glycol, water, and Ethanol. The brass nanoparticles synthesized are then prepared for conductive ink in printed electronics applications.

1.2 Objective of the research

The objectives of this research are to investigate the synthesis brass nanoparticles by arc discharge method and to study the effect of different dielectric liquids, amounts of metal loading, and concentration of reducing agents on size, morphology, structure, composition and oxidation stability of alloy nanoparticles synthesized.

1.3 Scope of the research

- 1.3.1 DC welding machine with 5 A. current is used.
- 1.3.2 The dielectric liquids used in submerged arc discharge system are ethylene glycol, DI water and ethanol. The temperatures of dielectric liquids are controlled by dry ice with ethylene glycol.
- 1.3.3 The amounts of brass loading are 3.47, 6.95, and 10.43 g/l.
- 1.3.4 L-ascorbic acid is used as a reducing agent.
- 1.3.5 The nanoparticles synthesized are printed on a substrate by screen-printing.

1.3.6 The nanoparticles synthesized are characterized by Transmission electron microscope (TEM), scanning electron microscope (SEM), and x-ray diffractometer (XRD).

1.4 Expected benefits

1.4.1 The optimum condition for synthesis of brass nanoparticles used in submerged arc discharge system.

1.4.2 The method to synthesize brass nanoparticles.

CHAPTER II

FUNDAMENTALS

2.1 Nanomaterials

Nanoparticles are the small object in 1-100 nm. In principle any collection of atoms bonded together with a structural radius of 1- 100 nm can be considered a nanoparticle. Nanoparticles are attractive because their properties depend on size and shape of particles. Some properties of nanoparticles are different from their bulk material that creates a new material with excellent properties. Nanoparticles often have special optical properties. They are small enough to confine their electrons and produce quantum effects. Example, nanoparticles show different colors from their microparticles, nanoparticles can melt at lower temperature than their larger particles. Other size-dependent property changes include quantum confinement in semiconductor particles, surface plasmon in some metal particles. Ferromagnetic materials smaller than 10 nm can switch their magnetisation direction using room temperature thermal energy, thus making them unsuitable for memory storage. In addition, nanoparticles can be sintered at lower temperatures than larger particles and required shorter time scales because of the high surface-to-volume ratio. Moreover, nanoparticles have been found to have some extra properties to apply in various applications.

2.2 Alloy

Alloy is multicomponent metallic that create an advanced material. They present very complex structures and properties. The range of properties of metallic systems can be greatly extended by taking mixtures of elements to generate intermetallic compounds or alloys. In many cases, there is an enhancement in specific properties upon alloying due to synergistic effects and the rich diversity of compositions, structures, and properties of metallic alloys has led to widespread applications in electronics, engineering, and catalysis.

2.3 Brass

Brass is an alloy of copper and zinc. Proportions of zinc and copper can be varied to create brass with different properties. Brass is the material of choice for equipment components in the electrical and engineering industry. Its specific properties can be used for special applications and longer life. The word "brass" covers a wide range of copper-zinc alloys with differing combinations of properties including strength, ductility, hardness, conductivity, machinability, wear resistance, color, corrosion resistance, recyclability. Combinations of these properties result in unique structural materials.

2.3.1 Property

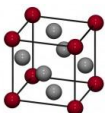
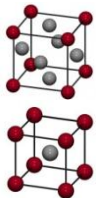
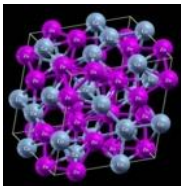
Brass is high malleability and low melting point (900 to 940 °C, 1652 to 1724 °F, depending on composition). Its flow characteristics make it a relatively easy material to cast. It can be hard or soft brasses depending on the compositions. The density of brass is approximately 0.303 lb/cubic inch, 8.4 to 8.73 grams per cubic centimeter.

Today almost 90% of all brass alloys are recycled. Because brass is not ferromagnetic, it can be separated from ferrous scrap by passing the scrap near a powerful magnet. Brass scrap is collected and transported to the foundry where it is melted and recast into billets. Billets are heated and extruded into the desired form and size.

2.3.2 type

A list of common brass alloys that is the mixture of copper and zinc, their chemical compositions and the uses of the different types of brass was summarized in table 2.1.

Table 2.1 the list of common brass alloys.

Brass type	%Zn	Structure	Property
Alpha brass	Less than 35	FCC 	It is malleable and can be worked cold. Generally, Alpha brass was used in pressing, forging, or similar applications. This brass can used in electrical applications such as alkaline battery anodes, fluorescent tube studs.
Alpha-beta brass	35–45	FCC&BCC 	It is suited for hot working. It contains both α and β' phase; the β' -phase is body-centered cubic and is harder and stronger than Alpha-beta.
Beta brass	45–50	BCC 	It can only be worked hot producing a hard strong metal that is suitable for casting.
Gamma brass	More than 50	Complex 	It is very brittle. It is not popular to use and unsuitable for general engineering purposes.

2.4 Electric arc discharge

In electric discharge machining, the metal was removed by means of electric spark erosion. The high temperature is created between a spark area and an electrode submerged in a dielectric liquid with the passage of electric current. The two electrodes are separated by a specific small gap called spark gap. The spark discharge happens in this gap with a dielectric media. Localized regions of high temperatures are formed due to the sparks occurring between the two electrode surfaces. Work piece material in this localized zone melts and vaporizes. Most of the molten and vaporized material is carried away from the inter-electrode gap by the dielectric flow in the form of particles. The particles are formed by two transformation stages nucleation and growth. To prevent excessive heating, electric power is supplied in the form of short pulses. Spark occurs wherever the gap between the tool and the work piece surface is smallest. After material is removed due to a spark, this gap increases and the location of the next spark shifts to a different point on the work piece surface. The schematic of electric discharge machining was shown in Fig. 2.1.

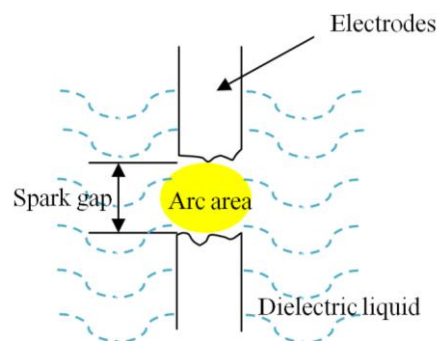


Figure 2.1 schematic of electric discharge machining.

2.5 Reduction-oxidation reaction

Reduction-oxidation or Redox reactions as Fig.2.2 are chemical reactions with the exchange of electrons between the reactant which leads to either some atom lose or gain electrons. An electron donor is reducer. An electron recipient is oxidizer. Thus reducers are "oxidized" by oxidizers and oxidizers are "reduced" by reducers.

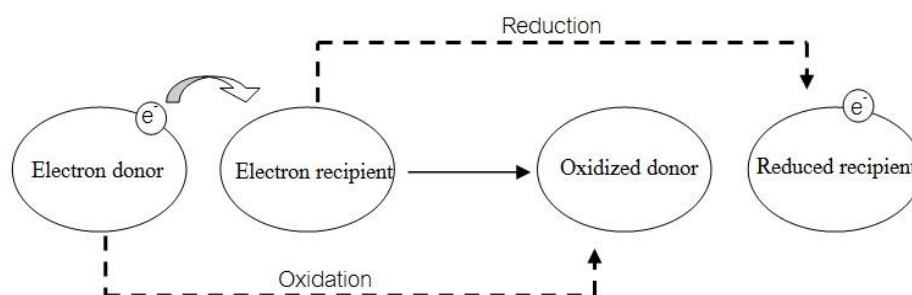
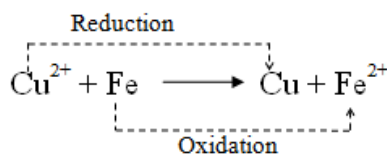


Figure 2.2 schematic of redox reaction.

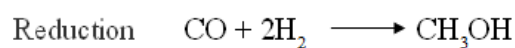
Redox reaction consists of two half-reactions: Oxidation and reduction. It can be explained in three terms.

- In term of electron transfer; Oxidation is loss of electron. Reduction is gain of electron.

Example;

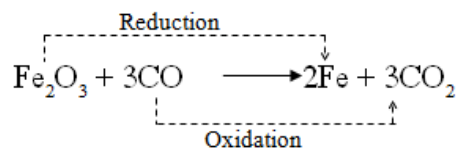


- In term of hydrogen transfer; Oxidation is loss of hydrogen. Reduction is gain of hydrogen. Example;



- In term of oxygen transfer; Oxidation is gain of oxygen. Reduction is loss of oxygen.

Example;



A reducing agent is the compound that donates electrons to another species in a reduction-oxidation (redox) reaction. A Good reducing agent often contains a low electro negativity atoms and low ionization energies such as ascorbic acid, formic acid.

An oxidizing agent is the compound that recipient electrons form another species in a reduction-oxidation (redox) reaction. It contains high electronegative atoms and even somemetals which have high oxidation numbers because it will gain electrons and be reduced such as halogens, potassium nitrate, and nitric acid.

2.5 Conductive inks

Conductive ink is ink that conducts electricity. It can be painted on a variety of materials. Conductive ink is a more economical way to create a conductive pattern when compared to traditional industry standards. Printing of conductive ink is a purely additive process producing little to no waste streams which then have to be recovered or treated.

Formulation of the conductive ink is crucial. The use of functional materials and nanoparticles in inks has broadened the scope of applications that printed electronics enables. They consist of nanometal, binder (an oil, resin or varnish of some kind), solvent and various additives such as drying and chelating agents. The exact recipe for a given ink depends on the type of surface that it will be printing on and the printing method that will be used. Conductive inks were designed to print by various printing methods on a wide range of subatrate such as metals, plastics and fabrics through to papers. The different types of conductive ink are produced to suit these different conditions.

2.6 Substrates

Printed electronics allows the use of flexible substrates, which lowers production costs and allows fabrication of mechanically flexible circuits. Key Challenges for substrates into print electronics applications are low shrinkage, low coefficient of thermal expansion, surface smoothness, solvent and moisture Resistance, and commercial availability. Other important substrate criteria are low roughness and suitable wettability, which can be tuned pre-treatment. In contrast to conventional printing, high absorbency is usually disadvantageous.

Substrates, used in printed electronic, have many type which suitable for different application. Example, inkjet and screen printing typically imprint rigid substrates like glass and silicon while mass-printing methods nearly exclusively use flexible foil and paper. A common choice substrate for printed electronic, Polyethylene terephthalate (PET) is low cost, high temperature stability, and chemical resistance for use in printed electronic. Polyimide (PI) is an alternatives substrate which very good heat resistance. It is used in the electronics industry for flexible cables, as an insulating film on magnet wire and for medical tubing. For example, in a laptop computer, the cable that connects the main logic board to the display (which must flex every time the laptop is opened or closed) is often a polyimide base with copper conductors. Paper's low costs and manifold applications make it an attractive substrate. However, its high roughness and large absorbency make it problematic for electronics.

2.7 Sintering

Sintering is the process of heating the particles to form a denser material. The main solid structure is developed from various types of mass transfer usually happens at the atomic level. Sintering can be said to the sintered diminishing porous between the particles. Starting with contraction of the connected components, then the particles grow together with a strong bond between the adjacent particles. Figure 2.3 shows developments of the microstructures by sintering.

- Initial sintering (Fig. 2.2 (b)) involving the rearrangement of the particles, neck formation only accounts for the first several percent of shrinkage and the particles begin pack together.
- Intermediate sintering stage (Fig. 2.2 (c)) occur when neck size enlarge and the pores decreases rapidly, because particles came in contact in great amount and align in a packed pattern. Grains and grain border are formed and increase in grain size. The process continues constantly while the pores merge and finally the pores starting to joined together which can cause particle relative density to rise.
- Final stage sintering (Fig. 2.2 (d)) occurs when pores joined and leave bulk solid by diffusion though grain border. The grain size is enlarged due to the sintering.

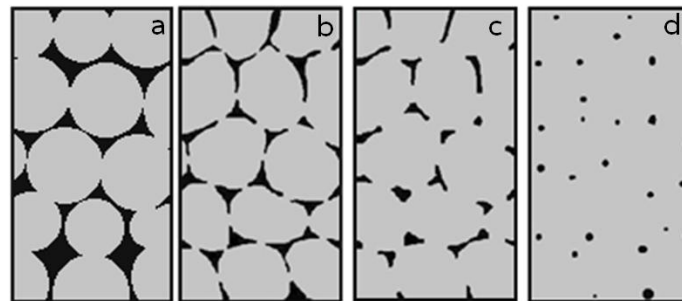


Figure 2.3 developments of the microstructures by sintering (a) Loose particle, (b) initial sintering, (c) intermediate sintering, (d) final state sintering.

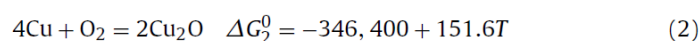
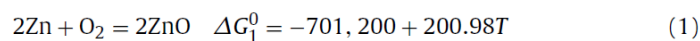
CHAPTER III

LITERATURE REVIEW

A major problem of the copper conductive ink is that copper oxides usually occur in ambient conditions. In order to protect the copper nanoparticles from oxidation, a number of approaches have been proposed. Xu et al. (2009) used electroless coating to synthesis Cu-Ag core-shell powder. They successfully synthesized silver coating on copper powder to protect copper from copper oxide but this method still high cost. Park et al. (2007) used PVP as capping agent and Jeong et al. (2011) used CTAP and PVP as co-capping agent. They found that the synthesized particles were pure copper without any oxide and the result shows bi-layer assembly at CTAB and PVP on copper surface. However, these coating material will hander inter-particle contact and hence conductivity unless removed in a subsequent sintering step.

In this work, Nanoalloy material is studied because some of its properties can be controlled by altering its composition. So we choose brass or copper-zinc alloy to solve the problems of copper oxide in the surface of copper powders. Many researchers reported about oxide on the surface of brass. Yun et al. (2004) investigated the effect of pulsed plasma oxidation on the corrosion resistance of brass. They used brass plate, which has a composition of Cu 65% and Zn 35%. After the plasma oxidation, the formation of ZnO was confirmed on the surface dominantly and α -brass sublayer was formed under the ZnO. The former is more thermodynamically stable for the oxides and the diffusivity of Zn is two to five times higher than that of Cu. Thermodynamically, it is impossible to synthesize relatively unstable Cu-oxides in ZnO layer.

Xu et al. (2010) studied the growth of ZnO nanostructure by thermal oxidation of brass ($\text{Cu}_{0.62}\text{Zn}_{0.38}$) foil at 400, 500, 600 and 700 °C in 5%O₂-N₂ at 1 atm. XRD pattern, Fig. 3.1, shows those low peak of ZnO are raised when the brass is oxidized at high temperature. Its do not show the peak of CuO, which can be explained by thermodynamics of alloy oxidation as equation below.



ΔG_0 is the free energy change when all species are present in their standard states. T is the absolute temperature. When temperature is 500 °C, ΔG_0 of formation for the solute metal oxide ZnO, -545,842 J, is more negative than that for the base metal oxide Cu₂O, -229,213 J. As a result, only external oxidation of Zn occurs.

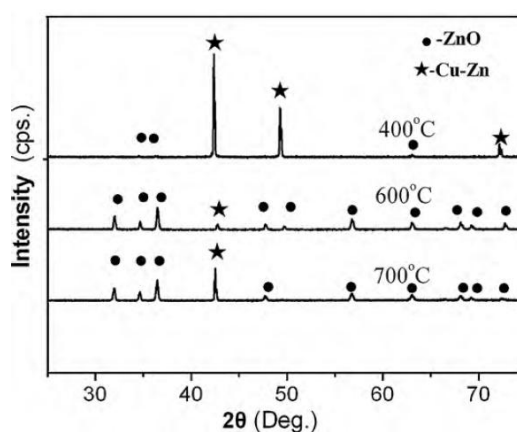


Figure 3.1 XRD spectra of oxide scale formed on the specimens after oxidation at different oxidation temperature for 3 h. showing that oxide is hexagonal ZnO.

Nanoalloy has been synthesized by many methods such as chemical reduction, electrochemical synthesis, electroless Coating. Farahmandjou et al. (2012), FePt nanoalloy was synthesized by chemical reduction of FeCl₂.4H₂O and Pt(acac)₂ at 250°C. FePt nanoparticles were successfully synthesized with mean diameter of 4 nm by polyol method. Yamauchi et al. (2012), Pt–Au alloys were synthesized by electrochemically. The alloys have been prepared using two sacrificial bulk metallic anodes in a single electrolysis cell. Bimetallic clusters of metals which are less soluble as anodes can be generated by electrochemically reducing their salts at the cathode.

For synthesis of nanobrass, the report of Pithawalla et al. (2003) synthesized 10-20 nm of Cu-Zn intermetallic by Laser based method for form long chain filament of Cu-Zn. The process involves pulsed laser to vaporized metal and condensed at low temperature with cooling pate. The products of this method are copper and brass nanoparticles. The formation of brass is Cu₅Zn₈ and CuZn₅. The average size of particles is 10-15 nm.

M.Z. Kassaei et al., 2008 synthesized nanobrass by arc discharge using brass rods (3mm×30 mm) submerged in various media at current 100 A for catalysts and support material application. In distilled water, both nanobrass (30 nm) and nano-Cu/ZnO (18 nm) are produced in comparable quantities. In gaseous nitrogen merely nanobrass (49 nm) is observed, in a high yield. In the open air, nanobrass (75 nm) is formed along with traces of ZnO. In ethylene glycol, nanobrass (108 nm) is formed as the major product along with a nanoalloy of CuZn₅ (25 nm). The smallest nanobrass is formed in water. The largest nanobrass is formed in ethylene glycol. Among these, distilled water proved to be the medium of choice for the arc synthesis of nanobrass.

The synthesis of nanoparticles by arc discharge method has been widely studied because of low cost, clean, and simple to produce. Moreover there are reports which were successful to prepare uniform novel nanoparticles. The main device of system is the power supply, two metal electrodes, servo control system to control speed rate of electrode, dielectric liquid. Arc discharge occurs between two electrodes with dielectric media, temperature during two electrodes will be high making the metal layers vaporize and condense into dielectric liquid.

Tien et al. (2010) synthesized silver and gold nanoparticles by arc discharge in deionized water. When the spark discharge occurs, hydrogen and oxygen atoms being imparted from water molecules. The reaction between the active atoms formed Ag-ion-like compound in water. In addition, the atoms of oxygen can adhere to the surface of Ag nanoparticles by hydrogen bond that why Ag nanoparticles can be suspended in water. As well as Au nanoparticles can be suspended in water without agglomeration because their surface bonded by oxygen atoms are supported by hydrogen bond with water. In conclusion Ag and Au nanoparticles can be a stable colloid without adding stabilizer because they are novel metal.

Tseng et al. (2009) synthesized gold ethanol colloid. The arc discharge system consists of servo control, magnetic stirrer, 25 °C of pure ethanol for dielectric media, two gold electrodes, power supply using 6.5 A 135 V for 3 min. This experiment used only pure ethanol as dielectric liquid to produce stable gold suspension. The particles size was found in 2-40 nm and can

suspended in ethanol without any surfactant. The experimental result of this research showed that the arc discharge technique is easy, cheap, clean method.

Lo et al. (2007) have been successfully synthesized silver nanofluid by the submerged arc discharge. They used 220 V., 7.5 A. of power supply and 2°C of deionized water as dielectric liquids. The synthesized nanofluid was characterized by UV-VIS and zetasizer. The average size of silver nanoparticles in deionized water is 6-25 nm.

Kassae et al. (2010) investigated an arc discharge synthesis as an effective method for direct preparation of high yields of nano-sized tungsten particles. The size, structure, purity, dispersion, and yield of W Nps are altered through variations of media and current (40–160 A). Gaseous nitrogen at 100 A offers rather smaller average sized and the purest W Nps. In such optimized conditions, TEM images show that the α -W Nps are predominantly spherical with a narrow particle size distribution and an average particle size of 68 nm. The β -W to α -W phase transformation varies with current, medium and particle size. The W Nps prepared by the arc discharge method may find wide applications in various fields such as electronics, illumination, cutting tools, anti-friction tools etc.

Other than this, there are more researches on effect of arc current and dielectric liquid to the particle aspect such as Lo et al. (2005) synthesized of copper by arc discharge using pure de-ionized water, 30%, 50%, 70% volume of ethylene glycol mixed with de-ionized water and pure ethylene glycol as dielectric liquid. XRD pattern of products can be indexed CuO, Cu₂O and Cu peak when dielectric liquid is de-ionized water because oxygen exists in de-ionized water. When the water percentage in solution decreases copper oxide also decreases. That means different dielectric liquid yield quite different structures.

Parkansky et al. (2006) synthesized nickel and carbon particles by pulsed arc between Ni electrodes submerged in ethanol. Using 99.5% of two Ni electrodes submerged in ethanol. One electrode with a 5 x 2.5 mm sparked with another 80 x 5 mm plate electrode at 100 Hz, amplitude

0.5 mm for 5 min. The production rate increases by increasing pulse energy and the size of particles increases with the pulse energy too.

Kassae, M.Z. and Buazar F. (2009) studied effect of media and current on the synthesis of Al nanoparticle by arc fabrication. They were investigated six different media including ethylene glycol, distilled water, liquid nitrogen, gaseous nitrogen, sunflower oil, and tap water. The results show that the sizes of Al nanoparticles in different media at 50 A are 26.6 nm in ethylene glycol, 30.0 nm in distilled water, 30.8 nm in liquid nitrogen, 33.1 nm in gaseous nitrogen, 34.9 nm in sunflower oil, and 40.9 nm in tap water. The particles in ethylene glycol are most dispersed and smallest size. And the current increases as the particles size increases. This research shows this method is a convenient, simplicity, low cost and high-purity.

Buazar et al. (2012) studied the synthesis of nanosteel by arc discharge and the effect of media and current on size, purity, yield and morphology of synthesized nanosteel. The media are nitrogen, open air, ethylene glycol, and distilled water saturated with polyvinylpyrrolidone (PVP). The synthesized particles in PVP-saturated distilled water and ethylene glycol are smaller than the synthesized particles in nitrogen and open air. When they changed current from 50 to 80 A/cm², the particles size in liquid media is decrease but the size is increase in gas media. The average nanoparticles size is 29 nm in nitrogen at 50 A/cm² and smaller 7 nm in distilled water at 100 A/cm² as the synthesized nanoparticles is a mixture of nanosteel and nano Fe₃O₄.

Hosseynizadeh et al. (2012) fabricated iron nanoparticles by arc discharge method in ethylene glycol and studied the effect of current on the size of nanoparticles. They are chosen ethylene glycol because the nanoparticles were stable in it and did not settle at the bottom of the container. The results show that the size of particles is about 103 nm at 10 A and it can raise the current leading to larger Nanoparticles.

In order to synthesis conductive ink for flexible electronic required low sintering temperature, high conductivity and low cost. There are many studies on solving this problem such as Kim et al. (2005), Prepared conductive ink from Ag particles to printed by ink-jet printing

followed by heat-treatment. They found that the Ag particles of small size are more reactive than the larger sized. Tai et al. (2010) Preparation of silver nanoink with 2 g of silver nano was dispersed in an aqueous medium. And use gel-ink pen to create conductive patterns.

Faddoul et al. (2012) prepared water-based silver ink contain 67-75% of silver particles. Conductive inks are a mixture of three parts including the conductive material, the inorganic binder and the vehicle. Then the ink was printed onto low temperature co-fired ceramic by screen printing. Schematic diagram of screening process is shown in Fig 3.2. The line of conductive tapes has 60 micrometer and $3 \times 10^{-8} \Omega\text{m}$ electrical resistivity. The patterns were sintered at 875°C under atmosphere. Their results show that electrical properties depended on silver content. Resistivity values varying from 1.6×10^{-8} to $3.3 \times 10^{-8} \Omega\text{m}$ were calculated over 36.3 cm line lengths.

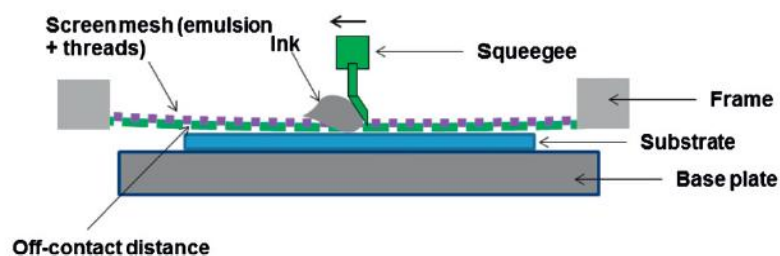


Figure 3.2 schematic of screen printing process.

CHAPTER IV

EXPERIMENTAL

4.1 Materials

- Brass wires (Cu 65%, Zn 53%)
- Ethylene glycol (QRëC)
- Deionization water
- Ethanol (VWR)
- Methanol (QRëC)
- Formic acid (QRëC)
- L-ascorbic acid (UNILAB)
- DC power supply (DC Inverter Arc welder, Iweld)
- Polyvinylpyrrolidone (PVP, K30 avg. Mw 40,000)
- Hydroxyethyl-cellulose (SIGMA)
- Coated PET film (Novacentrix)
- Screen frame

4.2 Synthesis of nanoparticles by arc discharge method

In this work, nanoparticles was synthesized by arc discharge brass wires submerged in three different dielectric liquid including deionized water, ethylene glycol, and ethanol. The schematic diagram of the system is shown in the Fig. 4.1. The system consists of brass wires (Cu 65%, Zn 35%, diameter 1 mm) as a cathode and anode electrode, DC power supply, controller feed seep of brass wire, dielectric liquid and cooling bath was used to control the temperature of the dielectric liquid.

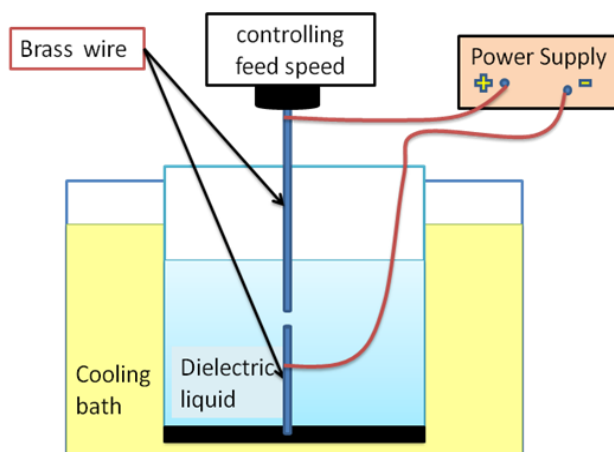


Figure 4.1 Schematic diagram of the arc discharge system.

4.2.1 Effect of dielectric liquid

First, brass wires were polished by sandpaper and washed with acetone. Then, the wires were connected to a cathode and anode electrode submerged in 80 ml of dielectric liquid. The temperature of the dielectric liquid was controlled by cooling bath as the condition in table 4.1. After the arc removed 3 centimetres of brass wires, the colloid solution was percolated by filter paper to remove the large particles. Next, the filtrate was separated by centrifuge 10,000 rpm at 25 °C for 20 min. Finally, the particles synthesized were washed with methanol and dried at 80 °C for 30 min.

Table 4.1 the experimental conditions to investigate effect of dielectric liquid.

Sample #	a	b	c
Amounts of brass loading (cm)	3	3	3
Dielectric liquid (80 ml)	DI water	Ethylene glycol	Ethanol
Cooling bath	Ice/water	Dry ice/ Ethylene glycol	Dry ice/ Ethylene glycol
Reducing agent	-	-	-
Voltage (Volts)	25.6	25.6	25.6
Current (Ampere)	5	5	5

4.2.2 Effect of reducing agent

The particles synthesized by arc discharge contain ZnO. Therefore, In order to convert ZnO to Zn particles. The effect of reducing agent were investigated, L-ascorbic acid was used. The colloid solution that synthesized by arc discharge was percolated by filter paper and added L-ascorbic acid. Next the colloid solution was separate by centrifuge 10,000 rpm at 25 °C for 20 min and washed with methanol. Finally, the synthesized particles were dried at 80 °C for 30 min. The experimental conditions to investigate the effect of reducing agent are shown in table 4.2.

Table 4.2 the experimental conditions to investigate the effect of reducing agent.

Sample #	a	b	c
Amounts of brass loading (cm)	3	3	3
Dielectric liquid (80 ml)	DI water	Ethylene glycol	Ethanol
Cooling bath	Ice/water	Dry ice/ Ethylene glycol	Dry ice/ Ethylene glycol
Reducing agent	Ascorbic â	Ascorbic â	Ascorbic â
Voltage (Volts)	25.6	25.6	25.6
Current (Ampere)	5	5	5

4.2.3 Effect of brass loading

When the concentration of particles in dielectric liquid increases, the new particles may coalesce with the particles suspended. The effect of brass loading was investigated. The particles were synthesized by arc discharge with different amount of brass loading including 3, 6, and 9 centimeters of brass wires submerged in 80 ml of ethylene glycol. The experimental conditions to investigate the effect of brass loading are shown in table 4.3.

Table 4.3 the experimental conditions to investigate effect of brass loading.

Sample #	a	b	c
Amounts of brass loading (cm)	3	6	9
Dielectric liquid (80 ml)	Ethylene glycol	Ethylene glycol	Ethylene glycol
Cooling bath	Dry ice/ Ethylene glycol	Dry ice/ Ethylene glycol	Dry ice/ Ethylene glycol
Reducing agent	Ascorbic â	Ascorbic â	Ascorbic â
Voltage (Volts)	25.6	25.6	25.6
Current (Ampere)	5	5	5

4.3 Preparation of conductive ink

1.125 liters of colloid solution, synthesized by arc discharge 9 centimeters of brass wires into 80 milliliters of ethylene glycol, was separated by centrifuge 10,000 rpm at 25 °C for 20 min and washed with Polyvinylpyrrolidone in methanol. Then, HEC and methanol were added into the separated particles and mixed.

4.4 Screen printing

The synthesized brass nanoparticles were dispersed in ink solution, then printed line pattern on substrate by screening printed and measured their resistivity.

In this work, the coated PET film was used as substrate. The schematic diagram of screen printing is shown in Fig. 4.2. First, Wooden frames are completely flat on the front surface of coated PET film. Then the brass ink was put on the gauzy curtain of frame. Next, the pattern was printed by immediately flooding with brass ink using a squeegee. Finally, the screen was moved into an upright position. The pattern was then dried at room temperature.

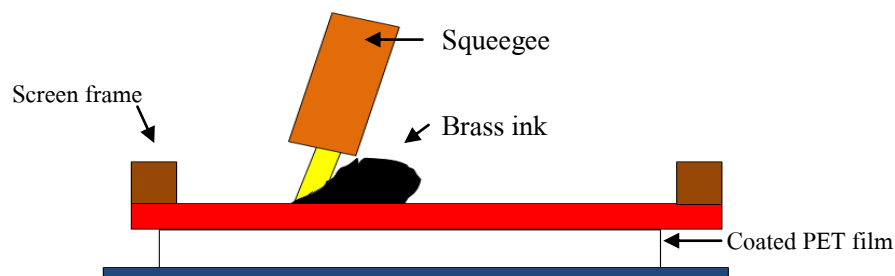


Figure 4.2 schematic diagram of screen printed.

4.5 Reactive sintering of formic acid vapor reduction

The brass pattern on coated PET substrate was heated at 150 °C with formic acid. Then, the effect of reactive sintering time on brass lines was investigated. The pattern was heat for 30, 60, 90, 120 and 480 min.

4.5 Characterizations

The particles synthesized were identified by scanning electron microscope (SEM) used to show external morphology, and crystalline structure. The SEM images are collected over a selected area of the surface of the sample in 2-dimensional. Areas ranging from approximately 1 cm to 2 microns in width can be imaged. Transmission electron microscopy (TEM) to analyzed the morphology and crystallize structure. TEM is a much higher spatial resolution than SEM, and can assist the analysis of features in the range of a few nanometers. X-ray diffraction (XRD) performs qualitative and quantitative analysis of polycrystalline materials.

After printed conductive ink on substrates, the patterns were identified by scanning electron microscope (SEM), X-ray diffraction (XRD) and measure their electric resistivity by two-point probe with LCR meter.

CHAPTER V
RESULTS AND DISCUSSIONS

5.1 Synthesis of Cu/Zn nanoparticles by arc discharge in different dielectric liquid

Nanoparticles were synthesized by arc discharge of brass wires submerged in three different dielectric liquids including deionized water, ethylene glycol, and ethanol. The brass rod was vaporized by the high temperature of the arc column and the metal vapor was then suddenly condensed by dielectric liquid at low temperature in order to generate clusters of nanoparticles. During the bombardment of spark discharge, hydrogen and oxygen atoms could imparted from dielectric liquid. Therefore, the particles synthesized can be metal or metal-oxide. Figure 5.1 shows the plasma and electrical discharge.

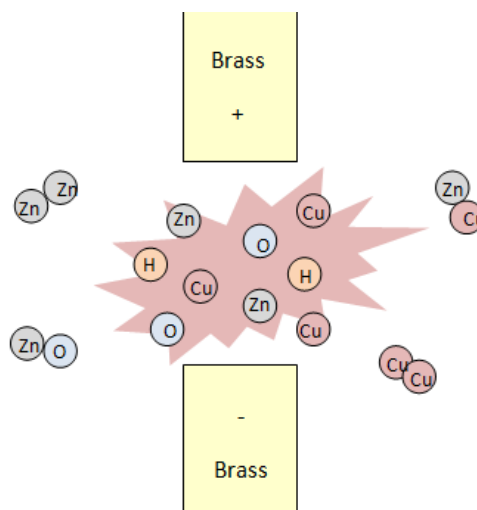


Figure 5.1 Plasma and electrical discharge.

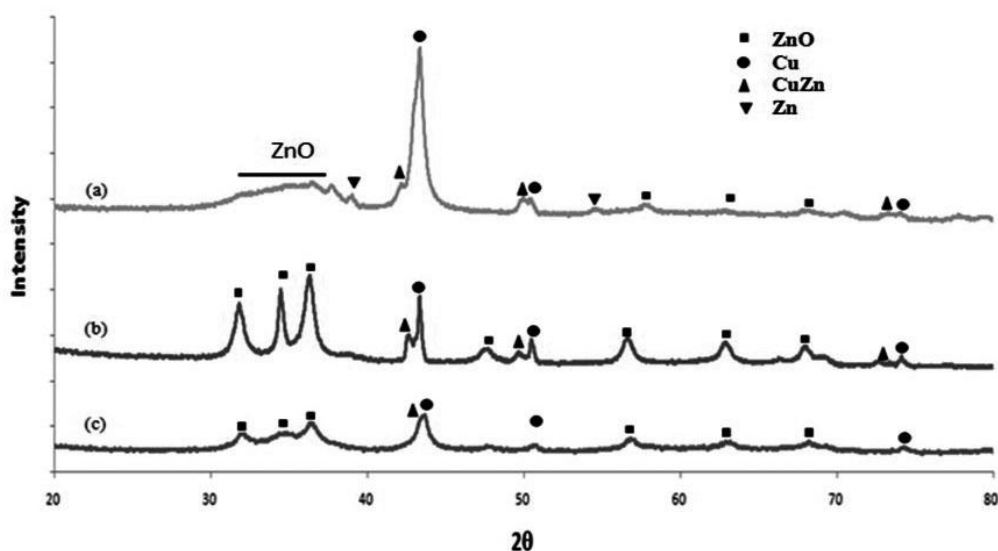


Figure 5.2 XRD patterns of nanoparticles synthesized in different dielectric liquids; (a) Ethanol, (b) Deionized water, (c) Ethylene glycol.

The XRD patterns of the nanoparticles synthesized in three dielectric liquids are shown in Fig. 5.2. The XRD pattern of the nanoparticles synthesized in ethanol shows the peaks of Cu (111), (200), (220), ZnO (100), (002), (101), (102), (110), (103), (112) Zn (110),(102) and CuZn (111), (200), (220). The XRD pattern of the nanoparticles synthesized in deionized water shows the peaks of Cu (111), (200), (220), ZnO (100), (002), (101), (102), (110), (103), (112) and CuZn (111), (200), (220). The XRD pattern of the nanoparticles synthesized in ethylene glycol shows the peaks of Cu (111), (200), (220), ZnO (100), (002), (101), (110), (103), (112) and CuZn (111).The XRD pattern of nanoparticles synthesized in ethylene glycol shows the peak of CuZn in a shoulder of copper peak. This adjacent peak overlaps copper peak and cannot be clearly separated because all particles are in nanocrystalline size. The XRD patterns of the nanoparticles in three dielectric liquids do not show the peak of CuO, because the standard electrode potential of copper ($E^0 = 0.34$ V) is higher than that of zinc ($E^0 = -0.76$ V). Therefore, ZnO are easier to be formed compared to CuO (Chung, 2004; Park, 2005). The average size of the nanoparticles synthesized in ethylene glycol, ethanol and deionized water estimated by Scherrer's equation were 10.9 nm, 17.3 nm, and 95.1 nm, respectively.

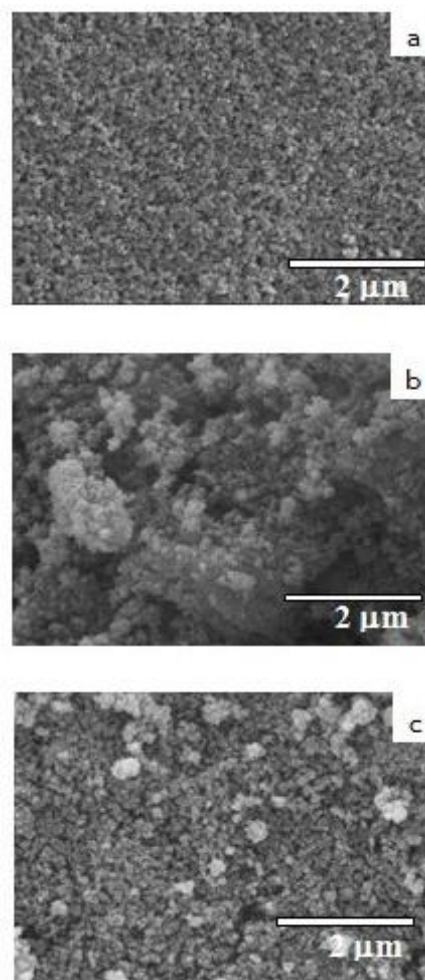


Figure 5.3 SEM image of nanoparticles synthesized in different dielectric liquids; (a) Ethanol, (b) Deionized water, (c) Ethylene glycol.

The SEM images in Fig. 5.3 show the morphology of the nanoparticles synthesized in different dielectric liquids. Figure 5.3(a) shows a uniform distribution of nanoparticles synthesized in ethanol. Figure 5.3(b) shows that the nanoparticles synthesized in deionized water were not uniformly distributed and wall compacted. Figure 5.3(c) shows the agglomerate of some nanoparticles synthesized by using ethylene glycol.

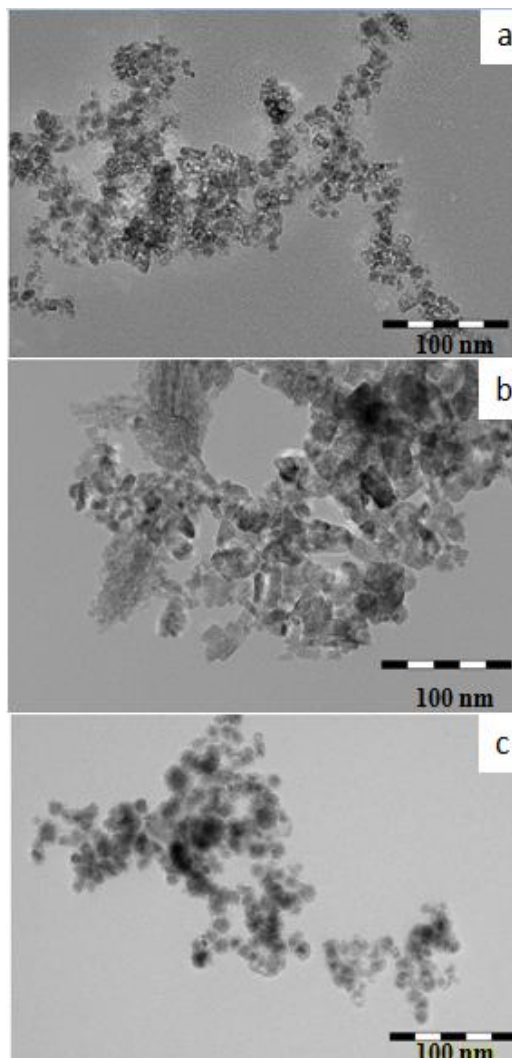


Figure 5.4 TEM images of nanoparticles synthesized in different dielectric liquids; (a) Ethanol, (b) Deionized water, (c) Ethylene glycol

The TEM images of the nanoparticles synthesized in different dielectric liquids are shown in Fig. 5.4. The TEM image of the nanoparticles synthesized in ethanol in Fig. 5.4(a) illustrates their spherical morphologies with 20 nm. Figure 5.4(b) shows the agglomeration of the large particles that synthesized in deionized water. Figure 5.4(c) shows the uniform spherical of particles synthesized in ethylene glycol with 15 nm.

The SEM and TEM images in Figs. 5.3 and 5.4 show that the morphology of the shape and size of the nanoparticles synthesized in three dielectric liquids are different. The first reason is that the temperatures of each dielectric liquid are different. We used ice mixed with water (0°C)

for cooling deionized water while the mixture of dry ice with ethylene glycol (-14°C) was used for cooling ethanol and ethylene glycol. The particle size depends on the difference temperature between arc column and dielectric liquid. Thus, the nanoparticles synthesized in deionized water are larger than the nanoparticles synthesized in ethanol and ethylene glycol.

The formation of the nanoparticles occurs in two stages. First, nucleation generated a critical nucleus. Second, growth of the critical nucleus to a larger size is formed. At the growth step, the growth rate depends on the competition between agglomeration and removal of the new nucleated. The size distribution of the nanoparticles synthesized is dependent on the growth process of the nuclei controlled by diffusion of the growth species from bulk to the growth surface as shown in Eq. 5.1. The size of particles decreases when diffusion coefficient decreases. Equation 5.2 shows that diffusion coefficient depends on temperature and viscosity of dielectric liquid. Therefore, dielectric liquids should have low temperature and high viscosity. The viscosity of ethylene glycol, ethanol and deionized water are 10.7, 0.88, 0.69 g/m.sec, respectively. Thus, the nanoparticles synthesized in ethylene glycol are smallest.

$$r^2 = 2D(C-C_s)V_m t + r_0^2 \quad (5.1)$$

$$D = kT/(2\pi\eta r) \quad (5.2)$$

Where r is the radius of spherical nucleus, D is the diffusion coefficient of the growth species, C is the bulk concentration in dielectric liquid, C_s is the concentration on the surface of solid particles, V_m is the molar volume of the nuclei, k is Boltzman constant, T is the temperature of dielectric liquid, and η is the viscosity of dielectric liquid.

The second reason that is dispersion stability that can be checked by a visual inspection of sedimentation (Kassae et al, 2009 and Hosseynizaded et al, 2012). The particles in deionized water are not well dispersed and settled at the bottom of the container. The low-volume compact mass is shown in the SEM image of the particles synthesized in deionized water (Fig. 5.3b). In addition, Ethylene glycol can act as a coating agent as well as weak reducing agent in order to protect the surface of the nanoparticles, hence smaller spherical particles can be obtained. The nanoparticles can suspend in ethylene glycol and do not settle without adding any stabilizer (Viau et al, 2003 and Chen et al, 2013).

5.2 Effect of reducing agents on the synthesized particles.

The nanoparticles synthesized by arc discharge contain ZnO. In order to convert ZnO to Zn, L-ascorbic acid was used as a reducing agent. Thus, the effects of L-ascorbic acid were investigated. Ascorbic acid was added into the colloid synthesized by arc discharge submerged in deionized water, ethylene glycol, and ethanol.

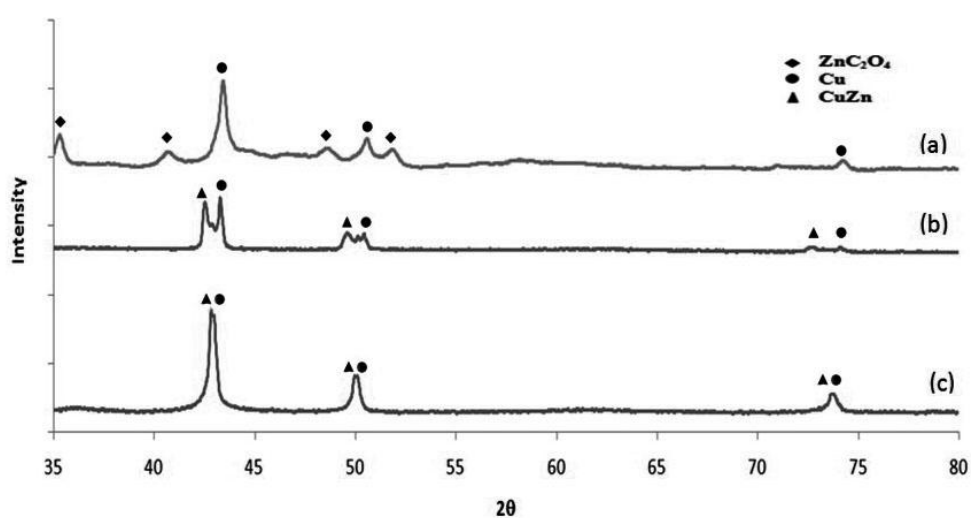


Figure 5.5 XRD patterns of particles synthesized in different dielectric liquids after adding ascorbic acid; (a) Ethanol, (b) Deionized water, (c) Ethylene glycol.

The XRD patterns of the particles synthesized in different dielectric liquids after adding ascorbic acid are shown in Fig. 5.5. The XRD pattern of the particles synthesized in ethanol (Fig. 5.5(a)) shows the peaks of Cu (111), (200), (220) and ZnC_2O_4 (021), (022), (421), (023). Zinc oxalate is attributed to the amount of hydrogen and oxalate ions in solvent, as ascorbic acid can be excessively converted to oxalates when free copper is very high (Kim et al., 2010 and Ni et al., 2011). The XRD pattern of the particles synthesized in deionized water (Fig. 5.5(b)) shows the peak of CuZn (111), (200), (220) and Cu (111), (200), (220). The XRD pattern of particles synthesized in ethylene glycol (Fig. 5.5(c)) shows the peak of CuZn (111), (200), (220) and Cu (111), (200), (220). By reacting with L-ascorbic acid, the XRD results of the particles synthesized in ethylene glycol and deionized water do not show the peak of ZnO because ZnO particles were completely reduced to zinc particles.

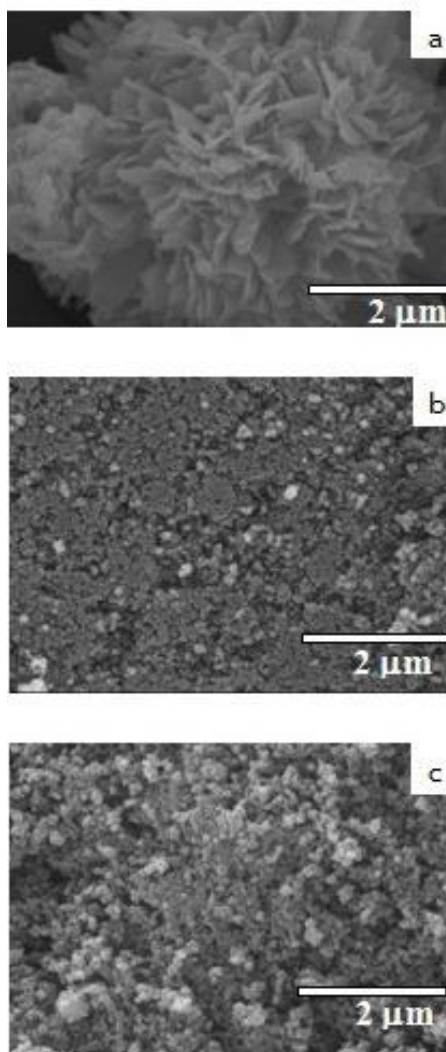


Figure 5.6 SEM image of particles synthesized in different dielectric liquids after adding ascorbic acid; (a) Ethanol, (b) Deionized water, (c) Ethylene glycol.

The SEM image of particles synthesized in ethanol in Fig. 5.6(a) illustrates the characteristics of the zinc oxalate. It was composed of nanosheets in a self-assembled structure (Kim et al., 2010; Ni et al., 2011). Figure 5.6(b) shows the compact particles synthesized in deionized water. Figure 5.6(c) shows the agglomerate of some nanoparticles synthesized in ethylene glycol.

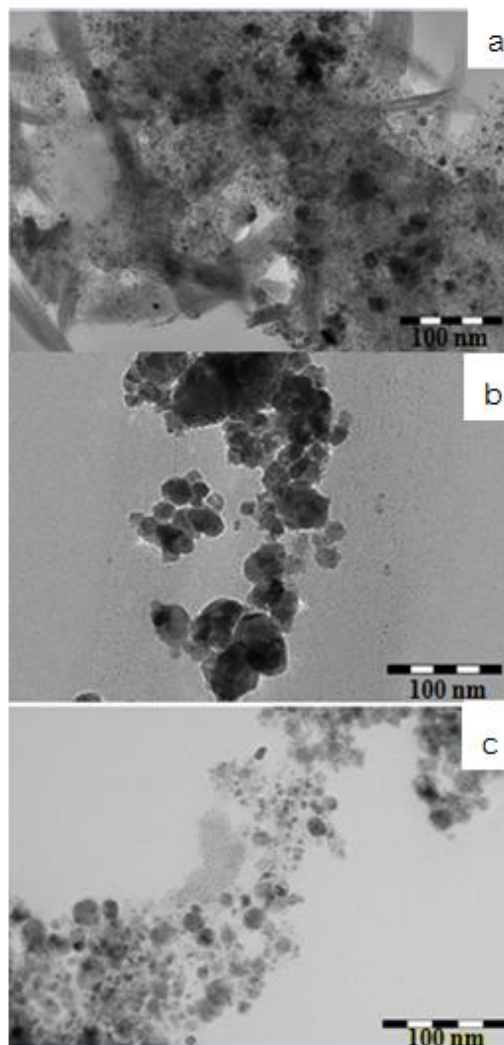


Figure 5.7 TEM images of particles synthesized in different dielectric liquids after adding ascorbic acid; (a) Ethanol, (b) Deionized water, (c) Ethylene glycol.

After adding ascorbic acid, TEM images of particles synthesized are shown in Fig. 5.7. The TEM image of particles synthesized in ethanol (Fig. 5.7(a)) illustrates the characteristics of the zinc oxalate. The size of particles synthesized in deionized water (Fig.5.7 (b)) was about 100 nm. The TEM image of particles synthesized in ethylene glycol (Fig. 5.7(c)) illustrates their spherical morphologies with 10-20 nm.

5.3 Effect of brass loading on the synthesized particles.

We used ethylene glycol (-14°C) as media and 0.1 M ascorbic acid as reducing agent. The effect of brass loading was investigated. Amounts of brass loading into ethylene glycol were 3.47, 6.95, 10.45 g/l. The concentration of colloid solutions were assayed by ICP spectrometer. The concentration of Cu and Zn in colloid solutions are shown in table 5.1. The XRD patterns of the particles obtained are shown in Figs. 5.8, 5.9. There shows the peaks of Cu, ZnO, and CuZn and no ZnO after adding ascorbic acid. The average size of the synthesized particles was estimated by the XRD peak using Scherrer's equation: 3.47 g/l (10.9 nm), 6.95 g/l (12.3 nm), 10.45 g/l (13.1 nm). The particles are slightly increases when amount of brass loading increases. The SEM and TEM image of the nanoparticles synthesized in different amount of brass loading are shown in Figs. 5.10 and 5.11. The SEM and TEM image show similar morphology.

Table 5.1 Amounts of brass loading into ethylene glycol and concentration of colloid solution.

Sample #	g	h	i
amounts of brass loading (cm)	3	6	9
Dielectric liquid (80 ml)	Ethylene glycol	Ethylene glycol	Ethylene glycol
amounts of brass loading (g/l)	3.47	6.95	10.43
Concentration of Cu in colloid solution (g/l)	0.28	0.49	0.57
Concentration of Zn in colloid solution (g/l)	1.15	2.29	3.77
Concentration of metal in colloid solution (g/l)	1.43	2.78	4.33
% yield	41.21	40	41.51

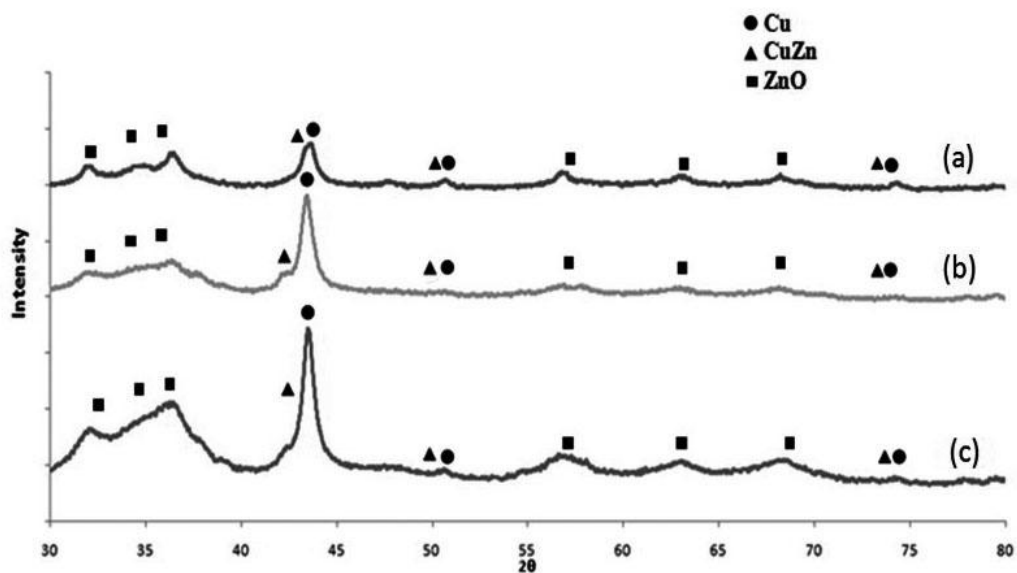


Figure 5.8 XRD patterns of the nanoparticles synthesized in different amount of brass loading; (a) 3.47, (b) 6.95, (c) 10.45 g/l.

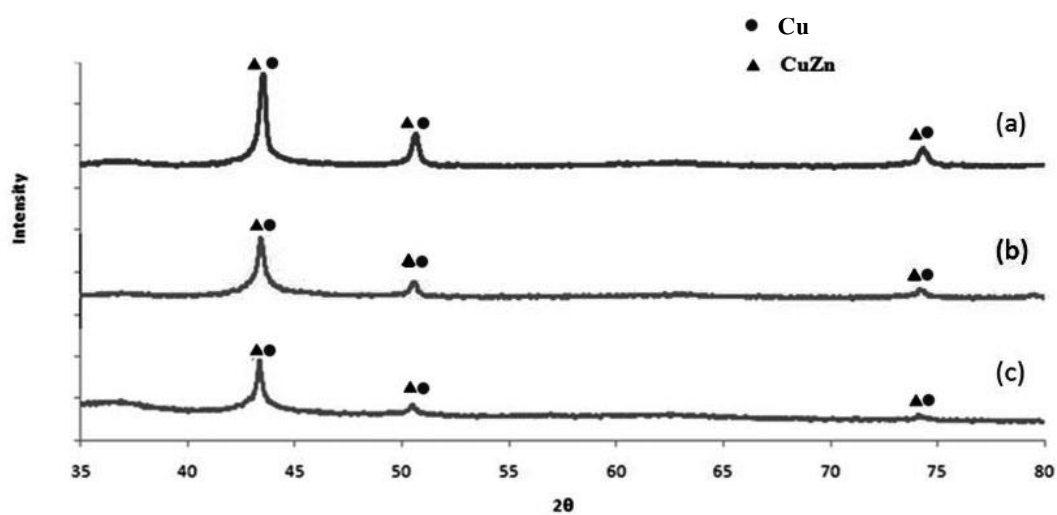


Figure 5.9 XRD patterns of the nanoparticles synthesized in different amount of brass loading after added ascorbic acid; (a) 3.47, (b) 6.95, (c) 10.45 g/l.

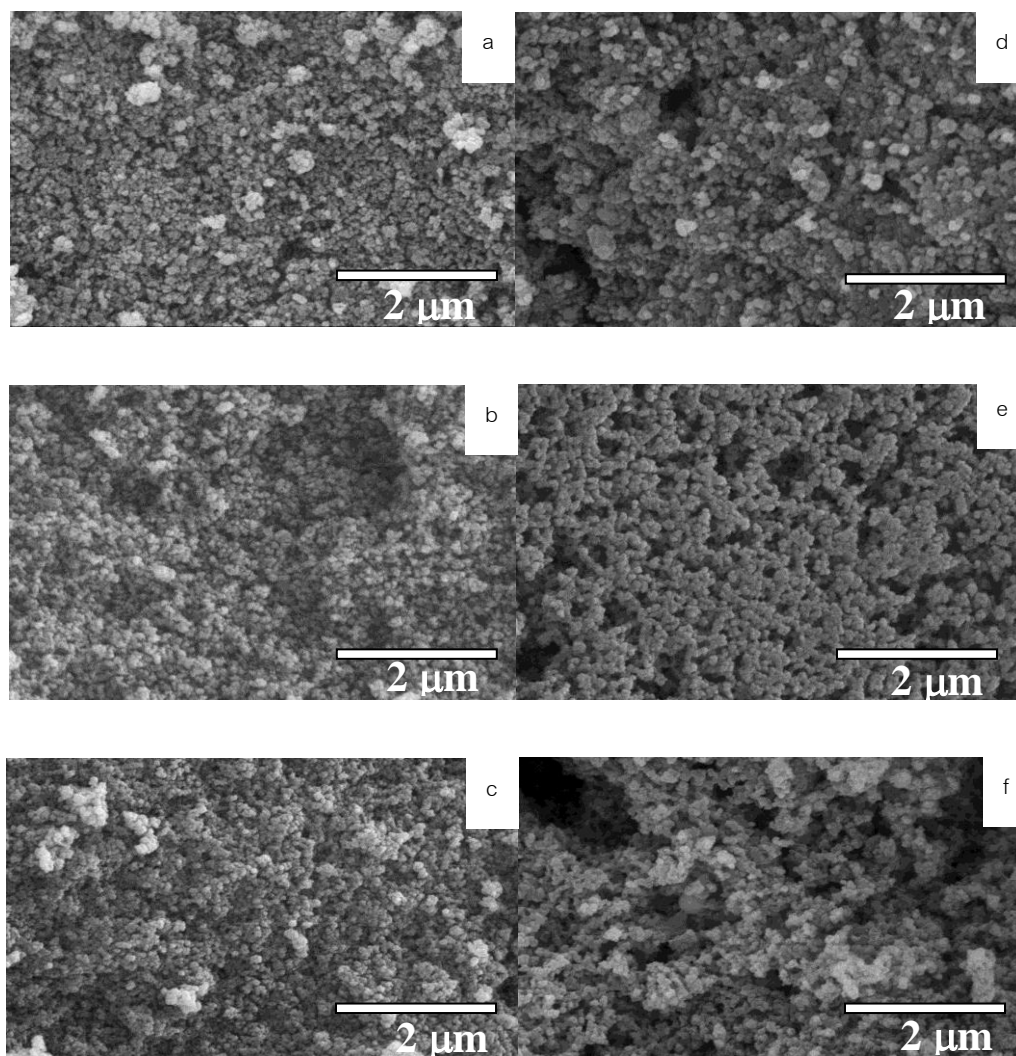


Figure 5.10 SEM image of the nanoparticles synthesized in different amount of brass loading; (a) 3.47, (b) 6.95, (c) 10.45 g/l and after adding ascorbic acid; (d) 3.47, (e) 6.95, (f) 10.45 g/l

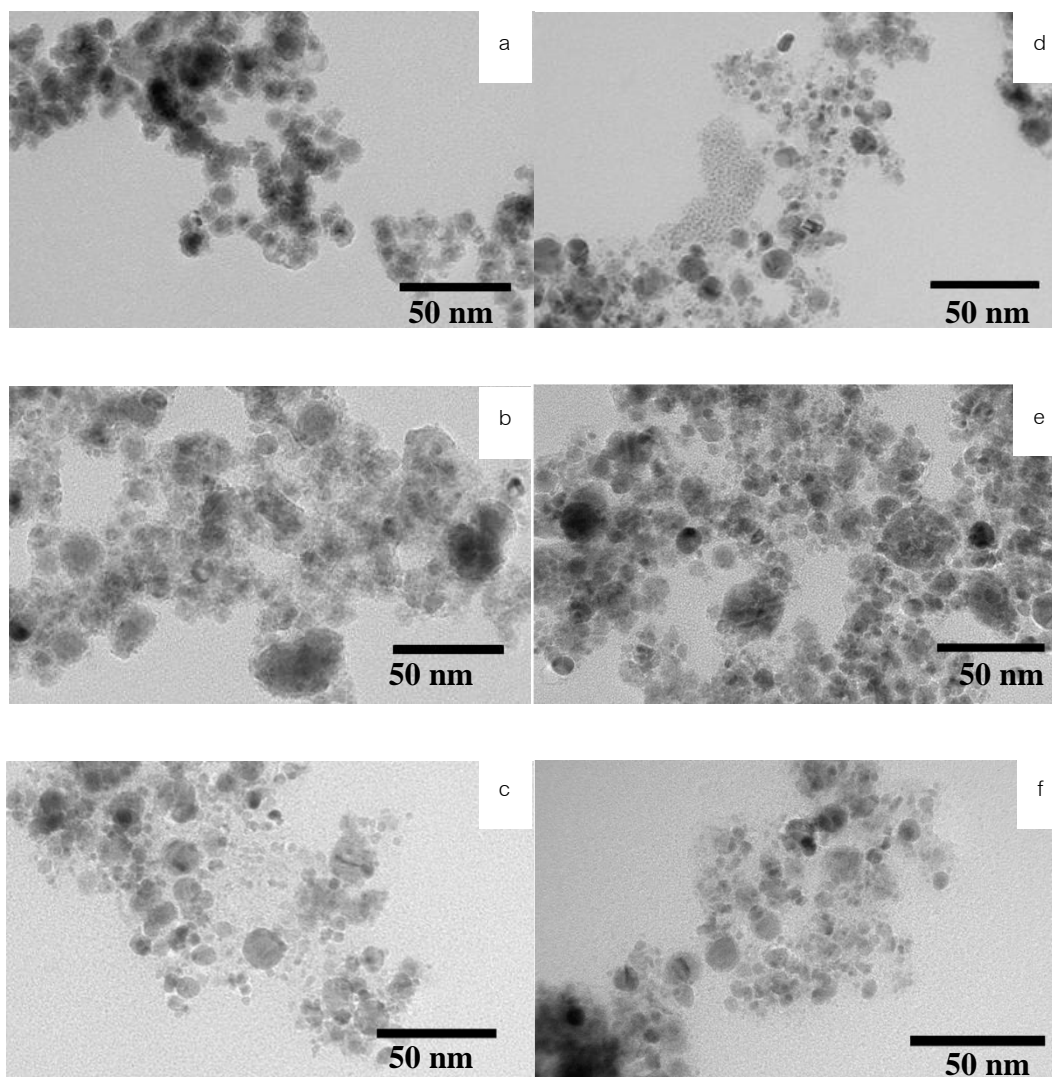


Figure 5.11 TEM image of the nanoparticles synthesized in different concentration of brass loading; (a) 3.47, (b) 6.95, (c) 10.45 g/l and after adding ascorbic acid; (d) 3.47, (e) 6.95, (f) 10.45 g/l

5.4 Printed and sintering processes

The Cu/Zn colloid solution previously synthesized was separated by centrifuge to obtain nanoparticles that is a main ingredient of a conductive ink. The obtained nanoparticles were mixed with other components including binder, and solvent. The compositions of each component are shown in table 5.2.

Table 5.2 the compositions of conductive ink.

Composition	%wt
Separated nanobrass	42.92
Methanol	36.70
Water	19.56
Hydroxyethyl-cellulose (HEC)	0.82

The conductive ink was homogenized by ultrasonic for 2 h. and then printed on PET substrates by screen printing. The printed pattern on coated PET film is shown in Fig. 5.12. After the pattern was dried at room temperature, the influence of reactive sintering by formic acid vapor at 150 °C on the conductive pattern was investigated.

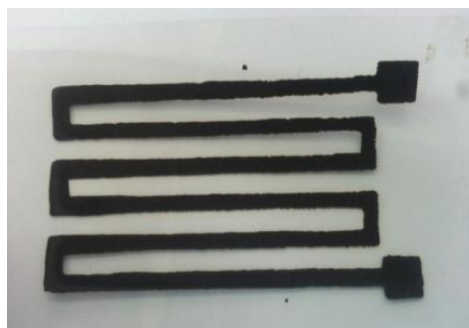


Figure 5.12 the screen printed pattern on coated PET substrate.

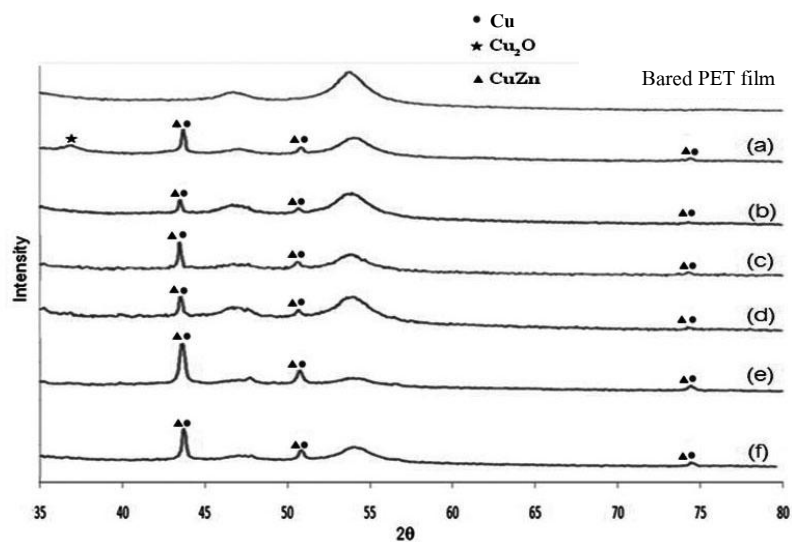
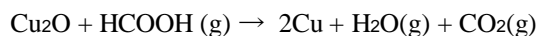


Figure 5.13 XRD pattern of the printed pattern on coated PET film (a) before sintering and after reactive sintering at 150 °C for; (b) 30 min, (c) 60 min, (d) 90 min, (e) 120 min, and (f) 480 min.

The XRD pattern of the printed pattern on coated PET film before reactive sintering, Fig. 5.13(a), demonstrate CuZn (111), (200), (220), Cu (111), (200), (220), and Cu₂O (110) that occur during the pattern dried at room temperature. After reactive sintering, Fig. 5.13(b-f), the XRD diffractions show the peak of CuZn and Cu. That mean Cu₂O can be removed by reactive sintering by formic acid vapor. The reduction reaction is presented in equation below (Yu, 2011; Schmeißer, 2011).



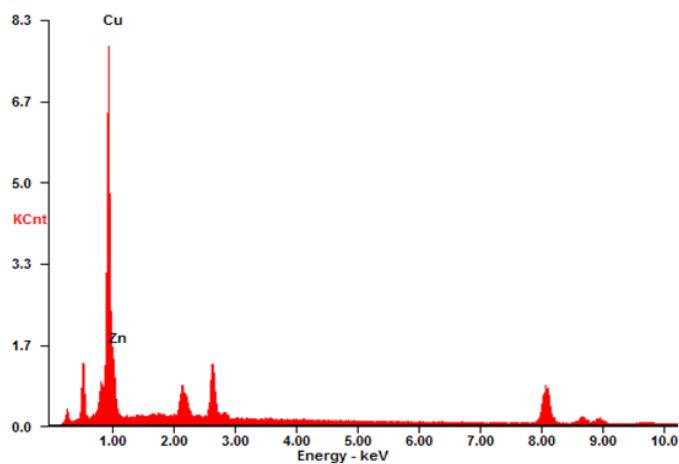


Figure 5.14 EDX pattern of the printed pattern on coated PET film.

Figure 5.14 shows the EDX of the printed pattern containing Cu 71%wt and Zn 29 %wt. The SEM images of the printed pattern on coated PET film followed by reactive sintering at 150 °C are shown in Fig 5.15. The particles begin melting after sintering for 30 min and could be clearly seen on the surface form to contiguous pattern at 480 min of sintering time. Meanwhile, the color of coated PET film began to change and deteriorate (Fig. 5.16).

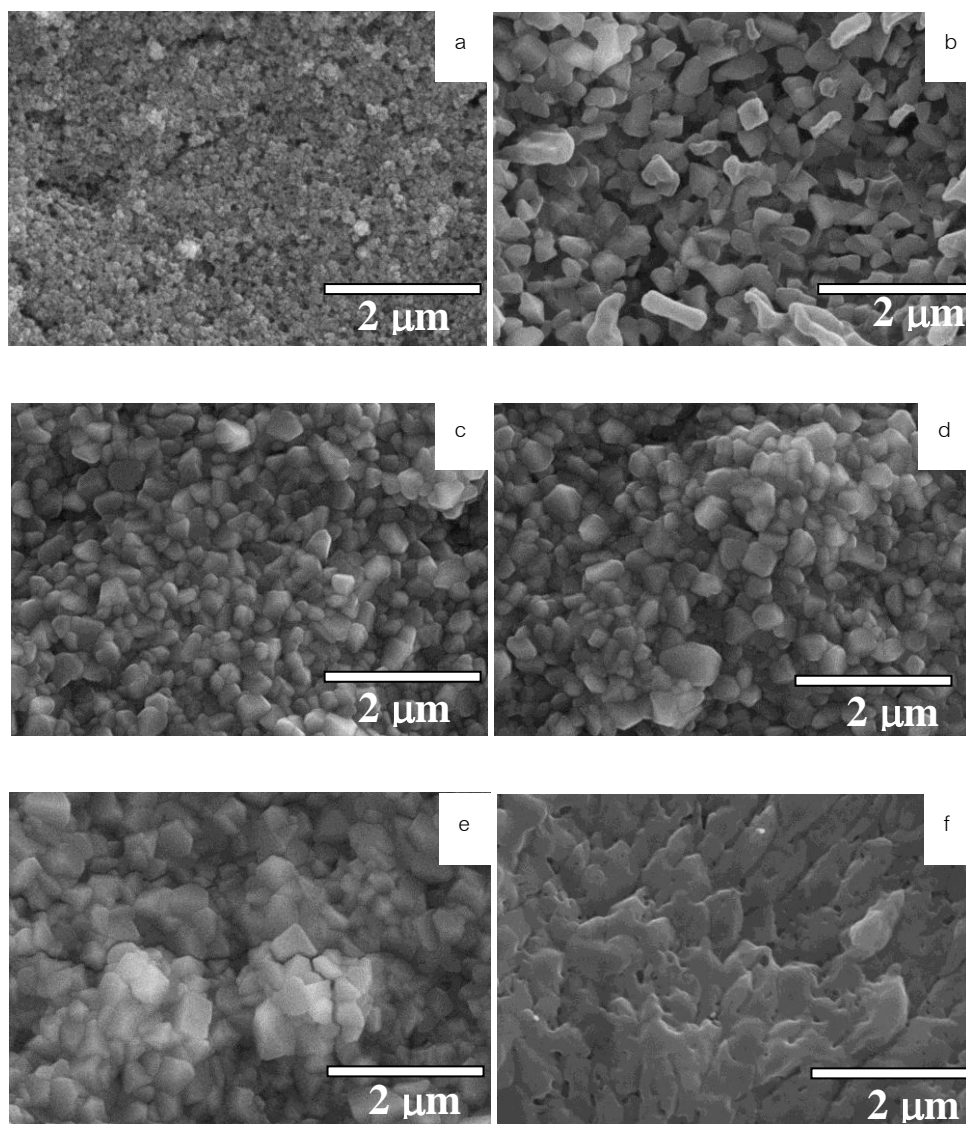


Figure 5.15 SEM images of the printed pattern on coated PET film (a) before sintering and after reactive sintering at 150 °C for; (b) 30 min, (c) 60 min, (d) 90 min, (e) 120 min, and (f) 480 min.

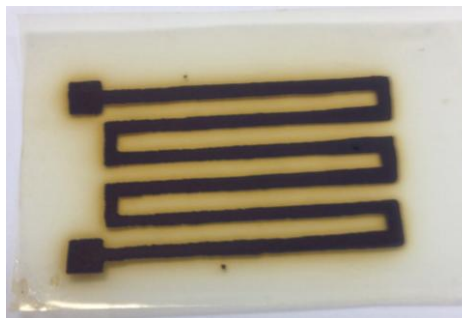


Figure 5.16 the printed pattern on coated PET film after sintering at 150 °C for 480 min.

The electrical resistivity of the printed pattern by reactive sintering for 30, 60, 90, 120 and 480 min are shown in table 5.3. The results show that the electrical resistivity decreases with the increase of the sintering time. Therefore, the reactive sintering by formic acid vapor reduction at 150 °C for 120 min is optimum condition to reduced Cu_2O and sintered the nanoparticles to continuous pattern. The electrical resistivity of the pattern after sintering for 120 is 24.28 Ωcm while the electrical resistivity of brass wire (Cu 65%, Zn 35%, diameter 1 mm) is $3.2 \times 10^{-4} \Omega\text{cm}$.

Table 5.3 the electric resistivity of the screen printed pattern using brass ink on coated PET substrate.

sample	Reactive sintering by formic acid vapor		Resistivity (Ωcm)
	Time (min)	Temperature ($^{\circ}\text{C}$)	
1	0	150	2413.35
2	30	150	36.12
3	60	150	34.60
4	90	150	33.85
5	120	150	24.28
6	480	150	22.05

CHAPTER VI

CONCLUSIONS

6.1 Summary of Results

Cu/CuZn nanoparticles were synthesized by arc discharge of brass wires submerged in three different dielectric liquid including deionized water, ethylene glycol, and ethanol. The XRD patterns of the nanoparticles synthesized in three dielectric liquids show the peaks of Cu, ZnO, and CuZn. The zinc oxide was formed by oxygen free radicals during decomposition of the dielectric liquid and the results do not show the peak of CuO because the standard electrode potential of copper is higher than that of zinc. Therefore, ZnO are easier to be formed compared to CuO. The average size of the nanoparticles synthesized in ethylene glycol, ethanol and deionized water estimated by Scherrer's equation were 10.9 nm, 17.3 nm, and 95.1 nm, respectively. That means type of dielectric liquid affects on size and morphology of particles obtained. L-ascorbic acid could reduce zinc oxide particles in deionized water and ethylene glycol. In ethanol, zinc oxalate was formed after adding ascorbic acid. The nanoparticles are slightly increased when amount of brass loading increases: 3.47 g/l (10.9 nm), 6.95 g/l (12.3 nm), 10.45 g/l (13.1 nm). Therefore, the synthesis of brass nanoparticles by arc discharge submerged in ethylene glycol with 10.45 g/l of brass loading and using L-ascorbic acid as reducing agent is optimum condition to synthesis of brass nanoparticles. The synthesized brass nanoparticles was dispersed in ink solution and printed on coated PET film by screen printing. The XRD pattern of the printed pattern demonstrates CuZn, Cu, and Cu₂O that occurs during the pattern dried at room temperature. Then, the printed pattern was sintered by formic acid vapor reduction. After reactive sintering, the XRD patterns show the peak of CuZn and Cu. That means Cu₂O can remove by reactive sintering by formic acid vapor. Furthermore, the electrical resistivity decreases with the increase of the sintering time. The reactive sintering with formic acid vapor at 150 °C for 120 min is optimum condition to reduce Cu₂O and sintered nanoparticles to continuous pattern. The electrical resistivity of the pattern after sintering for 120 min is 24.28 Ωcm.

6.2. Recommendations

1. The optimum percentage of zinc in brass, which can protect the occurrence of copper oxide and decrease the electrical resistivity of brass line, should be studied
2. The effect of binder and capping agent on conductivity of conductive ink should be studied.
3. The particles synthesized in ethanol are uniformly distributed and easy to separate, so the effect of other reducing agent, such as NaHB_4 , NaH_2PO_4 , should be studied.

REFERENCES

- Amirat, M., Zaidi, H., Djama, A., Necib, D., and Eyidi, D. 2009. Influence of the gas environment on the transferred film of the brass (Cu64Zn36)/steel AISI 1045 couple. Journal of wear 267: 433-440
- Ashkarran, A.A., Irajizad, A., Mahdavi, S.M., Ahadian, M.M., and Nezhad, M. 2009. Rapid and efficient synthesis of colloidal gold nanoparticles by arc discharge method. Journal of materials science and processing 96: 423-428.
- Bari, P., Rode, S., Duduke, A., Shinde, P., and Srivastav, V. 2012. Dielectric fluid in electro discharge machining. Proceeding of the NCNTE-2012: 109-114.
- Buazar, F., Cheshmehkani, A., and Kassaei, M.Z. 2012. Nanosteel synthesis via arc discharge: media and current effects. Journal of iranian chemical society 9: 151-156.
- Chen, Y., Liu, L., Wang, Y., Liu, J., and Zhang, R. 2011. Microstructure evaluation and thermal expansion of Cu-Zn alloy after high pressure heat treatment. Transactions of nonferrous metals society of china 21: 2205-2209.
- Chung, Y., Jung, M., Lee, S., Han, J., Park C., Ahn, S., and Kim J. 2004. A study of pulsed plasma oxidation effects on the corrosion resistance of brass. Journal of surface & coatings technology 188: 473– 477.
- Chung, Y.M., Jung, M.J., Lee, S.J., Han, J.G., Park, C.G., Ahn, S.H., and Kim, J.G. 2005. A study of plasma oxidation effects on the passive layer synthesis for the corrosion resistance of ($\alpha + \beta$) brass. Journal of surface and coatings technology 193: 243-248.

- Faddoul, R., Reverdy-Bruas, N., and Blayo, A. 2012. Formulation and screen printing of water based conductive flake silver pastes onto green ceramic tapes for electronic application. Journal of materials science and engineering 177: 1053-1066.
- Faddoul, R., Reverdy-Bruas, N., Blayo, A., Haas, T., Zeilmann, C. 2012. Optimisation of silver paste for flexography printing on LICC substrate. Journal of microelectronics reliability 52: 1483-1491.
- Farahmandjou M. 2012. Shape and composition study of iron-platinum (FePt) nanoalloy prepared by polyol process. Journal of physical sciences 7: 1938 – 1942.
- Gialanella, S. and Lutterotti, L. 2001. Metastable structures in α - β' brass, Journal of alloy and compounds 317: 479-484.
- Hosseynizadeh, S., Yazdani, A., and Khordad, R. 2012. Pure iron nanoparticles prepared by electric arc discharge method in ethylene glycol. Journal of applied physics 59: 30401.
- Jeong, S., Song, H.C., Lee, W.W., Lee, S.S., Choi, Y., Son, W., Kim, E.D., P, C.H., Oh, S.H., and Ryu, H.R. 2011. Stable aqueous based cu nanoparticles ink for printing well-defined highly conductive features and plastic subatrate. Langmuir 27: 3144-3149.
- Kamyshny, A., Steinke, J., and Magdassi, S. 2011. Metal-based inkjet inks for printed electronics. The open applied physics journal 4: 19-36.
- Kassae, M.Z., and Buazar, F. 2009. Al nanoparticles: Impact of media and current on the arc fabrication. Journal of manufacturing processes 11: 31-37.
- Kassae, M. Z., Buazar, F., and Motamedi1, E. 2010. Effects of current on arc fabrication of Cu nanoparticles. Journal of nanoparticles 10: 21-26.

- Kassaei, M. Z., Motamedi, E., Majidi, M., Cheshmehkani, A., Soleimani-Amiri, S. and Buazar, F. 2008. Media effects on nanobrass arc fabrications. Journal of alloy and compounds 453: 229-232.
- Kassaei, M.Z., Soleimani-Amiri, S., and Buazar, F. 2010. Diverse tungsten nanoparticles via arc discharge. Journal of manufacturing process 12: 85-91.
- Kim, D. and Moon, J. 2005. Highly conductive ink jet printed films of nanosilver particles for printable electronics. Journal of electrochemical and solid-state 8(11): j30-j33.
- Kim, N.S., Hwang, S.Y, Kim, E.Y. and Hah, K.N. 2010. Synthesis of Copper Nano-Ink in Alcohol Media. Journal of applied physics 49: 05EA04.
- Kim, S.J., Kim, Y.T., and Choi, J. 2010. Facile and rapid synthesis of zinc oxalate nanowires and their decomposition into zinc oxide nanowires. Journal of Crystal Growth 312: 2946–2951
- Liz-Marzan, L.M., 2004 Materialstoday. pp 26-31. spain: Univeersidade.
- Lo, C., Tsung, T. and Chen, L. 2005. Shape-controlled synthesis of Cu-based nanofluid using submerged arc nanoparticles synthesis system (SANSS). Journal of crystal growth 277: 636-642.
- Lo, C., Tsung, T., and Lin, H. 2007. Preparation of silver nanofluid by the submerged arc nanoparticle synthesis system (SANSS). Journal of alloys and compounds 434–435: 659–662.
- Mindivan, H., Çimenoglu, H., and Kayali, E.S. 2003. Microstructures and wear properties of brass synchroniser rings. Journal of wear 254: 532–537.

- Mukhopadhyay, N.K., Mukherjee, D., Bera, S., Manna, I., and Manna, R. 2008. Synthesis and characterization of nano-structured Cu-Zn γ -brass alloy. Journal of materials science and engineering 485: 673-680.
- Ni, L., Wang, L., Shao, B., Wang, Y., Zhang, W., and Jiang, Y. 2011. Synthesis of flower-like zinc-oxalate microspheres in ether-water bilayer refluxing systems and their conversion. Journal of material science technology 27(6): 563-569.
- Park, B.K., Jeong, S., Kim, D., Moon, J., Lim, S., and Kim, J.S. 2007. Synthesis and size control of monodispers copper nanoparticles by polyol method. Journal of colloid and interface science 311(2): 417-424
- Park, C., Kim, J., Chung, Y., Han, J., Ahn, S., and Lee, C., 2005. A study on corrosion characterization of plasma oxidized 65/35 brass with various frequencies. Journal of surface and coating technology 200: 77-82
- Parkansky, N., Frenkel, G., Alterkop, B., Boxman, R.L., Goldsmith, S., Barkay, Z., Rosenberg, Yu., and Goldstein, O. 2006. Influence of pulsed arc parameters on powder production in ethanol. Journal of powder technology 162: 121-125.
- Pithawalla, Y.B., El-Shall, M.S. and Deevi, S. 2003. Laser based synthesis of intermetallic Cu-Zn nanoparticles and filaments. Journal of scripta materialia 48: 671-676.
- Rui, X., Zhou, K., and Hu, M. 2009. Preparation of Core-shell Cu-Ag Bimetallic Powder via Electroless Coating. Journal of Wuhan university of technology-Mater: 637-639
- Russo, A., Ahn, B.Y., Adams, J.J., Duoss, E.B., Bernhard, J.T., and Lewis, J.A. 2011. Pen-on-Paper Flexible Electronics. Journal of Advanced Materials 23: 3426-3430.
- Schmeißer, M. 2011. Reduction of Copper Oxide by Formic Acid an ab-initio study. pp 3-8.

Germany: Chemnitz university of technology.

- Shim, I.K., Lee, Y., and Lee, K.J.. 2008. An organometallic route to highly monodispersed silver nanoparticles and their application to ink-jet printing. Materials chemistry and physics 110: 316–321
- Singh, A.K., Viswanath, V., and Janu, V.C. 2009. Synthesis, effect of capping agent, structural, optical and photoluminescence properties of ZnO nanoparticles. Journal of luminescence 129: 874-878
- Sridevi, D. and Rajendran, K.V. 2009. Synthesis and optical characteristics of ZnO nanocrystals. Bulletin materials science 32: 165-168.
- Tai, Y. and Yang, Z. 2011. Preparation of stable aqueous conductive ink with silver nanoflakes and its application on paper-based flexible electronics. Journal of surface interface analysis 44: 529-534.
- Tang, X.F., Yang, Z.G., and Wang, W.J. 2010. A simple way of preparing high-concentration and high-purity nano copper colloid for conductive ink in inkjet printing technology. Colloids and surfaces A: physicochemical and engineering aspects 360: 99-104.
- Tien, D.C., Chen, L.C., Thai, N.V. and Ashraf, S. 2010. Study of Ag and Au nanoparticles synthesized by arc discharge in deionized water. Journal of nanomaterial 10: 110-119.
- Tseng, K., Huang, J., Liao, C., Tien, Y. and Tsung, T. 2009. Preparation of gold ethanol colloid by the arc discharge method. Journal of alloy and compounds 472: 446-450.
- Viau, G., Brayner, R., Poul, L., Chakroune, N., and Lacaze, E., Fievet-Vincennt, F., Fievet, F. 2003. Ruthenium nanoparticles: size, shape, and self-Assemblies. Journal of chemical material 15: 486-494.

- Xu, C.H., Zhu, Z.B., Li, G.L., Xu, W.R., and Huang, H.X. 2010. Growth of ZnO nanostructure on Cu_{0.62}Zn_{0.38} brass foils by thermal oxidation. Journal of materials chemistry and physics 124: 252–256.
- Yamauchi, Y., Tonegawa, A., Komatsu, M., Wang, H., Wang, L., Nemoto, Y., Suzuki, N., and Kuroda, K. 2012. Electrochemical Synthesis of Mesoporous Pt–Au Binary Alloys with Tunable Compositions for Enhancement of Electrochemical Performance. Journal of american chemical society 134: 5100-5109.
- Yin, M., Wu, C.K., Lou, Y., Burda, C., Koberstein, J.T., Zhu, Y., and O'Brien, S. 2005. Copper Oxide Nanocrystals. Journal of american chemical society 127: 9506-9511.
- Yu, E.K., Piao, L., and Kim S.H. 2011. Sintering Behavior of Copper Nanoparticles. The bulletin of the korean chemical society 32: 4099-4102

VITA

Miss Rachawee Savanglaa was born on May 4th, 1989 in Bangkok, Thailand.
She received the Bachelor Degree of Chemical Engineering from Thammasat University 2010.
She continued her education in chemical engineering at Chulalongkorn University.